Optimal Operation of Islanded AC/DC Hybrid Microgrids: Supplementary Information

Arif Ahmed
Email: arif.ahmed@tum-create.edu.sg

1 Nomenclature

DG	Distributed Generator
$P^{ac}_{G_i}$	Active power generation by DG^{ac}_i at bus i in the AC subgrid
$Q^{ac}_{G_i}$	Reactive power generation by DG^{ac}_i at bus i in the AC subgrid
f, f_0	f is the system frequency, f_0 is the no-load frequency
f_{max_i}, f_{min_i}	Maximum and minimum frequency of DG^{ac}_i at bus i in the AC subgrid
P_{rated_i}, Q_{rated_i}	Rated active and reactive power generation of DG^{ac}_i at bus i in the AC subgrid
$\lvert V^{ac}_i\rvert$	Voltage magnitude of bus i in the AC subgrid
$\lvert V^{ac}_0\rvert$	No-load voltage magnitude in the AC subgrid
$\lvert V^{ac}_{max_i}\rvert, \lvert V^{ac}_{min_i}\rvert$	Maximum and minimum voltage magnitude of DG^{ac}_i at bus i in the AC subgrid
$K^{ac}_{P_i}$	Active power droop gain of DG^{ac}_i at bus i in the AC subgrid
$K^{ac}_{Q_i}$	Reactive power droop gain of DG^{ac}_i at bus i in the AC subgrid
$\boldsymbol{I^{ac}}$	Current injection vector of the AC subgrid
$\boldsymbol{V^{ac}}$	Bus voltage vector of the AC subgrid
$\boldsymbol{Y}$	Admittance matrix of the AC subgrid
V^{dc}_i	Voltage magnitude of bus i in the DC subgrid
V^{dc}_0	No-load voltage magnitude in the DC subgrid
$K^{dc}_{I_i}$	I-V droop gain of DG^{dc}_i at bus i in the DC subgrid
$K^{dc}_{P_i}$	Active power droop gain of DG^{dc}_i at bus i in the DC subgrid
$I^{dc}_{G_i}$	Current injection of DG^{dc}_i at bus i in the DC subgrid
$P^{dc}_{G_i}$	Active power generation of DG^{dc}_i at bus i in the DC subgrid
$\boldsymbol{I^{dc}}$	Current injection vector of the DC subgrid
$\boldsymbol{V^{dc}}$	Bus voltage vector of the DC subgrid
$\boldsymbol{G}$	Conductance matrix of the DC subgrid
f_{lol}	Level of loading in the AC subgrid
$f^{dc}_{lol_j}$	Level of loading of bus j in the DC subgrid
$V^{dc}_{max_i}, V^{dc}_{min_i}$	Maximum and minimum voltage magnitude of buses in the DC subgrid
$C^{ac}_{DG_i}(P^{ac}_{G_i})$	Cost of generation due to DG^{ac}_i at bus i in the AC subgrid
P_{ic_i}	Active power flow via interlinking converter i
K^{ic}_P	Interlinking converter droop gain
$P^{ac}_{L_i}$	Active power load at bus i in the AC subgrid
δ_i	Voltage angle of bus i in the AC subgrid
$G^{ac}_{ik}(f)$	Real part of the AC subgrid admittance element (i,k) at frequency f
$B^{ac}_{ik}(f)$	Imaginary part of the AC subgrid admittance element (i,k) at frequency f
$Q^{ac}_{L_i}$	Reactive power load at bus i in the AC subgrid
$P^{dc}_{G_i}$	Active power generation by DG^{dc}_i at bus i in the DC subgrid
$C^{dc}_{DG_i}(P^{dc}_{G_i})$	Cost of generation due to DG^{dc}_i at bus i in the DC subgrid
$P^{dc}_{L_i}$	Active power load at bus i in the DC subgrid
G^{dc}_{ik}	Element (i,k) of the DC subgrid conductance matrix
$S^{ac}_{G_i}$	Apparent power generation by DG^{ac}_i at bus i in the AC subgrid
$\mathcal{N}_{\mathrm{ac}}$	Set of AC buses
$\mathcal{N}_{\mathrm{dc}}$	Set of DC buses
$\mathcal{G}_{\mathrm{ac}}$	Set of DGs in the AC subgrid
$\mathcal{G}_{\mathrm{dc}}$	Set of DGs in the DC subgrid
$\mathcal{C}_{\mathrm{ic}}$	Set of Interlinking Converters

2 Cost Function of DGs

The quadratic cost function of DG_1^{ac} connected at Bus 1 in AC subgrid is:

$$C_{DG_1}^{ac}(P_{G_1}^{ac}) = 140 + 6.3P_{G_1}^{ac} + 0.005(P_{G_1}^{ac})^2 \qquad (\text{¢/h}) \tag{1}$$

The quadratic cost function of DG_3^{ac} connected at Bus 3 in AC subgrid is:

$$C_{DG_3}^{ac}(P_{G_3}^{ac}) = 200 + 10P_{G_3}^{ac} + 0.008(P_{G_3}^{ac})^2 \qquad (\text{¢/h}) \tag{2}$$

The quadratic cost function of DG_3^{dc} connected at Bus 3 in DC subgrid is:

$$C_{DG_3}^{dc}(P_{G_3}^{dc}) = 160 + 7P_{G_3}^{dc} + 0.008(P_{G_3}^{dc})^2 \qquad (\text{¢/h}) \tag{3}$$

The quadratic cost function of DG_6^{dc} connected at Bus 6 in DC subgrid is:

$$C_{DG_6}^{dc}(P_{G_6}^{dc}) = 160 + 5P_{G_6}^{dc} + 0.005(P_{G_6}^{dc})^2 \qquad (\text{¢/h}) \tag{4}$$

3 Parameter Values and Constraint Limits - Optimization

AC and DC Grid no-load voltage is 230V.
AC grid no-load frequency is 50 Hz.

For DG_1^{ac}:

$$-15 \text{ kW} \leq P_{G_1}^{ac} \leq 15 \text{ kW} \tag{5}$$

$$-10 \text{ kVAR} \leq Q_{G_1}^{ac} \leq 10 \text{ kVAR} \tag{6}$$

$$(S_{G_1}^{ac})_{max} = 18.75 \text{ kVA} \tag{7}$$

For DG_3^{ac}:

$$-20 \text{ kW} \leq P_{G_3}^{ac} \leq 20 \text{ kW} \tag{8}$$

$$-15 \text{ kVAR} \leq Q_{G_3}^{ac} \leq 15 \text{ kVAR} \tag{9}$$

$$(S_{G_3}^{ac})_{max} = 25 \text{ kVA} \tag{10}$$

For DG_3^{dc}:

$$-20 \text{ kW} \leq P_{G_3}^{dc} \leq 20 \text{ kW} \tag{11}$$

For DG_6^{dc}:

$$-15 \text{ kW} \leq P_{G_6}^{dc} \leq 15 \text{ kW} \tag{12}$$

For Interlinking Converter:

$$-10 \text{ kW} \leq P_{ic} \leq 10 \text{ kW} \tag{13}$$

For all AC subgrid buses:

$$218.5 \text{ V} \leq |V_i^{ac}| \leq 241.5 \text{ V} \qquad \forall i \in \mathcal{N}_{\text{ac}} \tag{14}$$

$$-\pi \leq \delta_i \leq \pi \qquad \forall i \in \mathcal{N}_{\text{ac}} \tag{15}$$

For all DC subgrid buses:

$$218.5 \text{ V} \leq |V_i^{dc}| \leq 241.5 \text{ V} \qquad \forall i \in \mathcal{N}_{\text{dc}} \tag{16}$$

System frequency:

$$47.5 \text{ Hz} \leq f \leq 52.5 \text{ Hz} \tag{17}$$

Refer next Section for load details.

Parameters	Value
Resistance	0.668 Ω/km
Reactance	0.879 Ω/km
Half Line Charging Susceptance	0.0005 Ω^{-1}/line
Line Lengths	100 m
$K_{P_1}^{ac}$	1.666e-4 (Hz/W)
$K_{P_3}^{ac}$	1.25e-4 (Hz/W)
$K_{Q_1}^{ac}$	1.15e-3 (V/VAR)
$K_{Q_3}^{ac}$	7.66e-4 (V/VAR)
Peak Load (for all loads)	5 kW + j3.75 kVAR

Table 1: 6-bus AC subgrid details.

Parameters	Value
Resistance	2.35 Ω/km
Line Lengths	100 m
$K_{P_3}^{dc}$	1.15e-3 (V/W)
$K_{P_6}^{dc}$	1.53e-4 (Hz/W)
Peak Load (for all loads)	5 kW

Table 2: 6-bus DC subgrid details.

4 12-bus AC/DC Hybrid Microgrid Details

The details regarding the AC subgrid follows:

The details regarding the DC subgrid follows:

The interlinking converter droop K_P^{ic} is 2e-4 $(1/W)$.

4.1 Load Profile

The loads in the microgrid follow the normalized load profile presented in Figure 1:

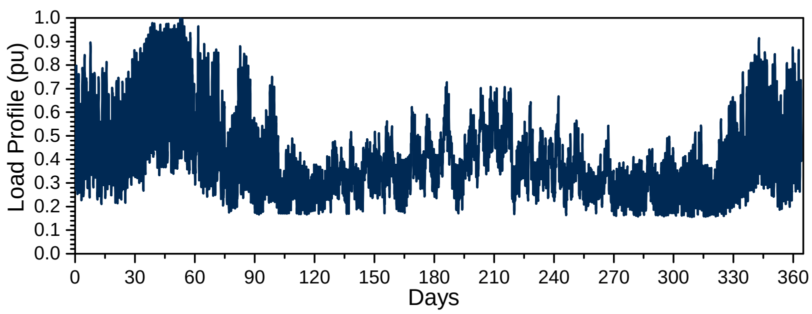

Figure 1: Normalized Load Profile in pu.

4.2 Solar Generation Profile

The solar PV generation profile is presented in Figure 2.
It should be noted that the solar generation in the network was considered at a power factor of 0.8 lagging.

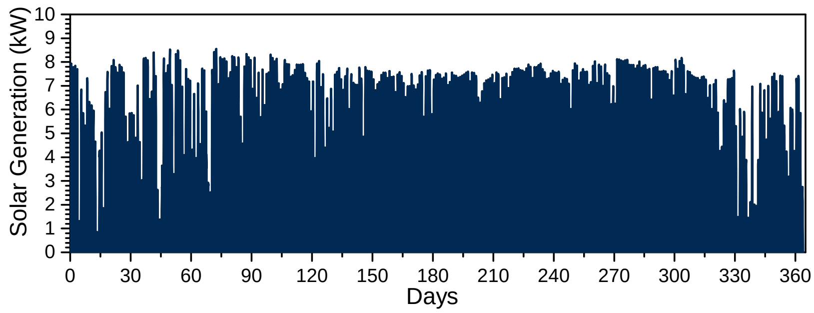

Figure 2: Solar PV Generation Profile in kW.

5 Additional Results

Figure 3 presents the frequency of the AC subgrid for the entire year. Figure 4 presents the network losses

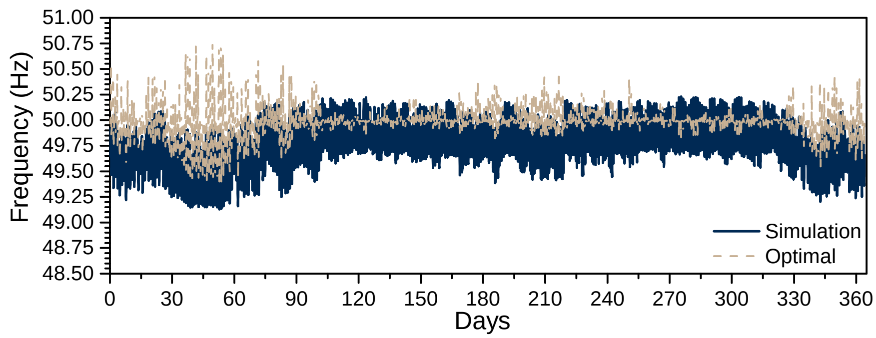

Figure 3: AC subgrid frequency in Hz.

(AC and DC) obtained via simulation, while Figure 5 presents them for the optimal case for the month of January.

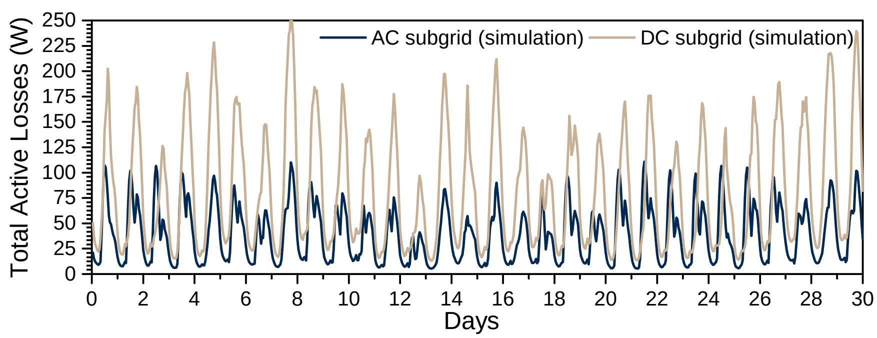

Figure 4: AC and DC subgrid losses in W.

Table 3 presents the cost per month via simulation, optimization, and the savings per month for the 12-bus AC/DC hybrid network.

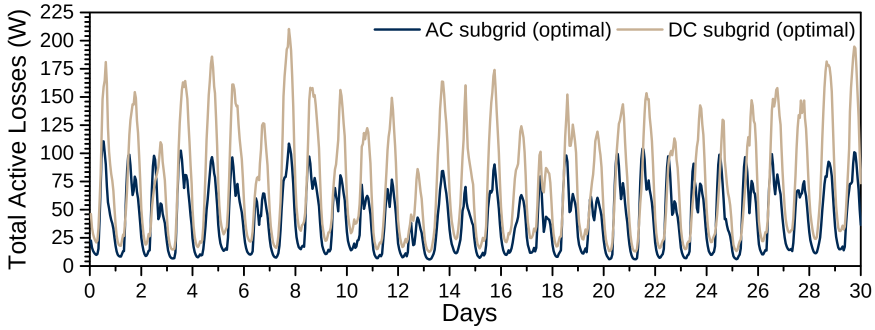

Figure 5: AC and DC subgrid optimal losses W.

Month	Cost (simulation) ($)	Cost (optimal) ($)	Savings per month ($)
January	5485.79	5452.17	33.61
February	5154.01	5112.14	41.87
March	5439.57	5411.24	28.32
April	5050.27	5037.76	12.50
May	5224.25	5210.44	13.81
June	5115.67	5099.39	16.28
July	5388.06	5365.07	22.99
August	5328.28	5309.33	18.94
September	5053.04	5040.16	12.87
October	5168.34	5158.63	9.703
November	5073.08	5056.31	16.76
December	5338.43	5302.32	36.11

Table 3: Cost savings per month in $.